

## Gypsum Scale Inhibition on Process Equipment Surfaces: A Review

Marina Prisciandaro<sup>a</sup>, Amedeo Lancia<sup>b</sup>, Dino Musmarra<sup>c</sup>,  
Giuseppe Mazziotti di Celso<sup>d</sup>

<sup>a</sup>Dipartimento di Ingegneria Industriale, dell'Informazione e di Economia, Università dell'Aquila, viale Giovanni Gronchi 18, 67100 L'Aquila, Italy

<sup>b</sup>Dipartimento di Ingegneria Chimica, dei Materiali e della Produzione Industriale, Università "Federico II" di Napoli, P. Le V. Tecchio, 80, 80125 Napoli, Italy

<sup>c</sup>Dipartimento di Ingegneria Civile, Design, Edilizia e Ambiente, Seconda Università degli Studi di Napoli, Real Casa dell'Annunziata, Via Roma 29, 81031 Aversa (CE), Italy

<sup>d</sup>Univ. of Teramo, Faculty of Bioscience, Via C. Lerici, 1, 64023 Mosciano S.A. (TE), Italy.  
marina.prisciandaro@univaq.it

The aim of the paper is to quantify and to compare the antiscalant effect of several additives on gypsum precipitation by measuring the retard on the induction period for nucleation. Through a well-assessed laser light scattering technique previously devised, the induction times are measured, and then used to estimate thermodynamic parameters such as the activation energy for nucleation, in a calcium sulfate supersaturated solution with the addition of NTMP, PBTC and citric acid. Experiments are carried out at a fixed additive concentration level (equal to 0.05 g/L), with the temperature varying in the range 15 – 35 °C. A comparison among different additives allows to define which is the most active in retarding gypsum scale formation.

### 1. Introduction

Gypsum scale deposition on process equipment surfaces has several disadvantages: in particular, when scales crystallize on heat transfer surfaces, they offer a resistance to the heat flow and they can accumulate in pipelines, orifices and other flow passages seriously impeding the process flow. Moreover, calcium sulfate scales, together with calcium carbonate scales, are the major cause of fouling in reverse osmosis membranes, resulting in a continuous decline in desalted water production thus reducing the overall efficiency and increasing operation and maintenance costs. Therefore, from an economic point of view, the formation of calcium sulfate mineral scales is an obstacle to the recovery of potable water from sea or brackish waters, as well as to the industrial utilization of many natural waters.

Calcium sulfate, CaSO<sub>4</sub>, has several forms, *i.e.* calcium sulfate dihydrate (commercially known as gypsum), calcium sulfate anhydrous (anhydrite), calcium sulfate hemihydrate, present in two different structures,  $\alpha$ -hemihydrate and  $\beta$ -hemihydrate (stucco or plaster of Paris). In natural deposits, the main form is the dehydrate; however, some anhydrite is also present in most areas, although to a lesser extent (Kirk-Othmer, 2011). Besides occurring naturally in the environment, calcium sulfate can be obtained by precipitation. In particular, calcium sulfate may crystallize as gypsum, calcium sulfate hemihydrate and anhydrite. In the recent years, there has been a revival of interest in calcium sulfate for biomedical applications, in which it is of great interest to synthesize uniform low-dimension crystals of calcium sulfate through wet chemical process (Sandhya et al., 2012). Gypsum is also obtained as a by-product of various chemical processes. The main sources are processes that involve gas scrubbing, *i.e.* burning sulfur-containing fuels, such as coal, used in electrical power generating plants, and the chemical synthesis of chemicals, such as sulfuric acid, phosphoric acid, titanium dioxide, citric acid, and organic polymers.

For all above mentioned question, the understanding of gypsum nucleation mechanism is of great importance in different fields. Despite the fact that considerable research has been going on over the past decades on the formation of calcium sulfate in aqueous media there is still some uncertainty as to the

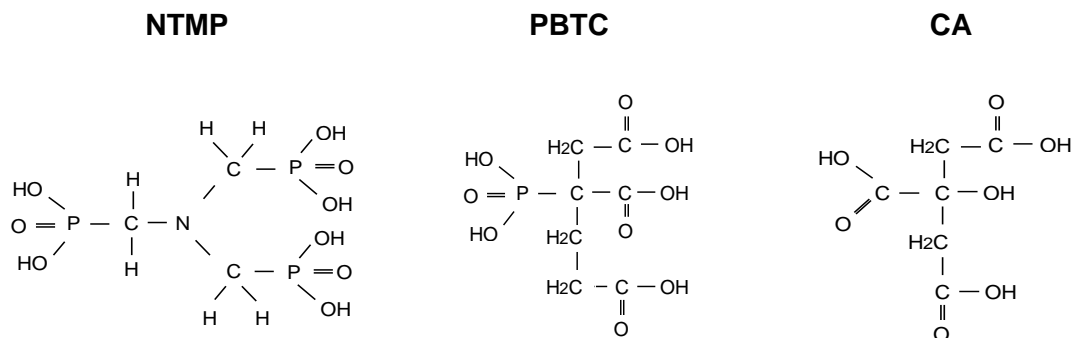


Figure 1: Structure of the three tested additives

mechanism of formation of this salt, because of the widely variable conditions of the solutions in which the salt formation takes place, including temperature, pH, ionic strength and composition and the presence of foreign ions and/or water soluble compounds (Lioliou et al., 2006). In the present paper, experimental results relative to the measurement of induction time for gypsum nucleation as a function of temperature are presented, with the addition in solution of several additives and namely citric acid (CA), NTMP, PBTC, whose structures are shown in Figure 1; they are able to retard the formation of gypsum nuclei, through the increasing of induction times.

### 1.1 Induction time measurement and nucleation mechanisms

The study of the effects of an additive on gypsum nucleation can be carried out by evaluating the induction period, defined as the time elapsing between the onset of supersaturation and the formation of critical nuclei, or embryos.

The various experimental techniques detect with a different resolution the first portions of the crystalline phase, that nucleates and grows in a supersaturated solution. As a result, under otherwise equal conditions, induction time may not have the same value when measured by different techniques.

However, this time primarily depends on solution supersaturation and temperature and it is the sum of two components: nucleation time ( $t_n$ ), related to the appearance of the critical nuclei, and growth time ( $t_g$ ), connected to the growth process, leading from critical nuclei to measurable crystals. Depending on the relative values of these two time periods, induction time can be influenced by nucleation alone ( $t_n \gg t_g$ , nucleation-controlled induction period), by both mechanisms ( $t_n \cong t_g$ , nucleation-and-growth-controlled induction period) or by growth alone ( $t_n \ll t_g$ , growth-controlled induction period) (Söhnel and Mullin, 1988). While  $t_g$  can be estimated by a kinetic growth expression,  $t_n$  is more difficult to quantify. Nevertheless, it is possible to discriminate whether the appearance of the new solid phase is controlled by nucleation and/or by growth, on the basis of the dependence of  $t_{ind}$  on supersaturation.

In particular, if the process which takes place is truly homogeneous nucleation, *i.e.* it occurs in a clear solution under the effect of supersaturation alone,  $t_{ind}$  is inversely proportional to the nucleation rate, defined as the number of nuclei formed in solution per unit time and volume.

In this case, as shown by Mullin (2001) and Söhnel and Garside (1992), it is possible to use the experimental knowledge of the induction period to estimate the activation energy ( $E_{act}$ ) for nucleation based on the dependence of  $t_{ind}$  on temperature.

Moreover,  $t_{ind}$  dependence on supersaturation allows to determine the interfacial tension ( $\gamma_{sl}$ ) between crystals and the surrounding solution.

In this paper, the three tested additives already compared to study their effect on gypsum interfacial tension (Prisciandaro et al., 2009), are now examined to evaluate their influence on activation energy.

## 2. Materials and Methods

The experimental apparatus consists of a stirred reactor with a related optical device and is schematically sketched in Figure 2. The reactor is a batch cylindrical crystallizer, made of glass, with a working volume of  $1.1 \times 10^{-3} \text{ m}^3$  and a diameter of 0.09 m. The crystallizer is surrounded by a water jacket for temperature control; stirring is provided by a two-blade polypropylene stirrer, with rotation rate ranging between 1 and  $10 \text{ s}^{-1}$ . An off-take tube, placed at half of the working height of the vessel, allows to remove samples of the suspension.

The stream removed by the off-take tube is sent, by a peristaltic pump, to an analysis flow-through cell, and then is conveyed again to the crystallizer. Since we are interested in induction time measurements, it is reasonable to think that crystal nuclei are so small that they are not damaged while passing through the pumping device, though located after that measurement cell; this assumption was indeed confirmed by optical microscope analysis. The cell, made of quartz, is  $7 \times 10^{-2}$  m long, with a square section of  $2.5 \times 10^{-5}$  m<sup>2</sup> and  $2.5 \times 10^{-3}$  m thickness. A 10 mW He-Ne laser beam ( $\lambda = 632.8$  nm) is focused on the cell, orthogonal to its walls; the beam, whose diameter is 2 mm, is vertically polarized. On the path of the laser beam, placed at  $45^\circ$  with respect to its direction, a beam splitter is provided in order to divide the laser beam into two parts; one is used to illuminate the measurement cell, while the other, collected by a photodiode, allows to check the stability and the intensity of the laser beam ( $I_o$ ). The signal of the scattered light ( $I_{sca}$ ) is collected by two lenses of focal 120 and 50 mm, at  $90^\circ$  with respect to the laser beam; this signal is sent, through a quartz optical fiber which ends on an interferential filter, to a photomultiplier tube, connected to a power supply with voltage variable in the range of 0 - 1,000 V. The signal of the transmitted light ( $I_{trans}$ ) is collected by a photodiode located beyond the cell, at  $0^\circ$  with respect to the laser beam. The two analogue signals of scattered and transmitted light, together with  $I_o$ , are collected by a recorder device.

Supersaturated solutions of calcium sulfate were prepared by mixing clear aqueous solutions of reagent-grade  $\text{CaCl}_2 \cdot 2\text{H}_2\text{O}$  and  $\text{Na}_2\text{SO}_4$  (Applichem, Darmstadt, Germany). The additive solutions were prepared by adding PBTC ( $\text{C}_7\text{H}_{11}\text{O}_9\text{P}$  as 50 %w/w solution in water, available under the commercial name of Bayhibit<sup>®</sup> AM kindly provided by Lanxess Deutschland GmbH, Leverkusen) to bidistilled water. The dissolved  $\text{Ca}^{2+}$  ion concentration was measured by ethylenediaminetetraacetic acid titration using Murexide (Applichem, Darmstadt, Germany) as an indicator, while the  $\text{SO}_4^{2-}$  ion concentration was measured by means of turbidity measurements carried out in a spectrophotometer (Hach model 2010). The phosphonate ion concentration was determined by converting it into the orthophosphate form with potassium persulfate and a UV lamp and analyzing the free orthophosphate by means of a spectrophotometer (Hach model 2010).

Once prepared, all the solutions were filtered, by using a  $0.45 \mu\text{m}$  filter (Millipore, HVLP 4700) and a vacuum pump (Vacubrand, MZ4C), in order to eliminate all foreign materials inevitably present in the solution, and then mixed directly into the reactor. The additive aqueous solution was added to the  $\text{Na}_2\text{SO}_4$  solution and then fed to the reactor. The equimolar concentration of  $\text{CaCl}_2 \cdot 2\text{H}_2\text{O}$  and  $\text{Na}_2\text{SO}_4$  in the reactor varied between 50 and  $290 \text{ mol/m}^3$ , while the additive concentration was 0.05 g/L in the reactor.

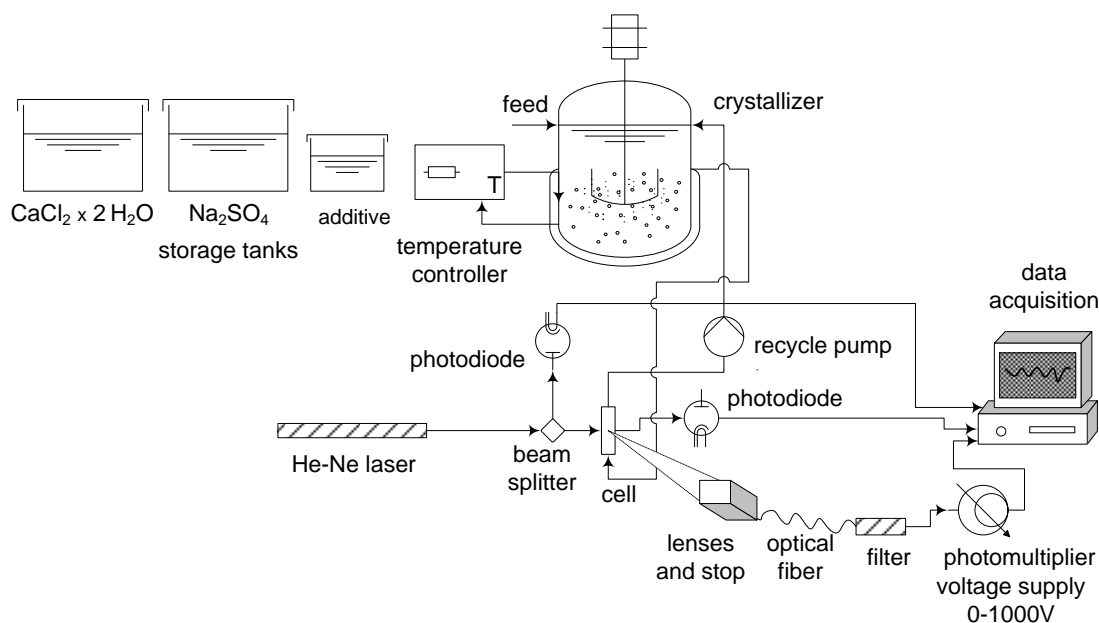


Figure 2: Sketch of the experimental apparatus used to measure the induction time

The additive concentration range was selected by considering the dosage range typically used as a scale inhibitor in industrial process equipment.

The supersaturation ratio  $S$  was calculated considering the liquid–solid equilibrium between  $\text{Ca}^{2+}$  and  $\text{SO}_4^{2-}$  ions and solid  $\text{CaSO}_4 \cdot 2\text{H}_2\text{O}$ , as described by the following equation:



so that it is:

$$S = \frac{a_{\text{Ca}^{2+}} a_{\text{SO}_4^{2-}} a_{\text{H}_2\text{O}}^2}{K_{ps}} \quad (2)$$

where  $a_J$  represents the activity of the  $J$  species ( $J = \text{Ca}^{2+}$ ,  $\text{SO}_4^{2-}$  and water) expressed as the product of the molality ( $m_J$ ) and the activity coefficient ( $\gamma_J$ ), and  $K_{ps}$  is the solubility product of gypsum. The value of  $K_{ps}$  was calculated as a function of temperature by means of the following relationship (Marshall and Slusher, 1966):

$$\ln(K_{ps}) = 390.96 - 152.62 \log T - 12545.62/T + 0.08T \quad (3)$$

The concentration values of the  $J$  species were calculated by solving a numerical model based on the equilibria that take place in the aqueous solution, and namely the acid dissolution equilibria of each additive, if present. The activity coefficients in the supersaturated solution were calculated by using a modified Debye–Hückel equation, as reported in a previous paper (Prisciandaro et al., 2006). All the experiments were carried out for a fixed value of additive concentration (0.05 g/L) while the supersaturation ratio changed in the range 2–5. The temperature was varied in the range 15–35 °C. The pH range varied in the interval 3.1–4.5. The induction period was evaluated by measuring the intensity of scattered and transmitted light signals as a function of time. These signals were processed to evaluate  $t_{ind}$  by adopting two parallel procedures, one graphical and the other one numerical. These procedures, described in detail elsewhere (Lancia et al., 1999), gave quite similar ( $\pm 10\%$ ) results.

### 3. Results and discussion

Experimental results can be grouped in two series: the first includes tests conducted by setting the temperature at the value  $T = 25$  °C, the additive concentration at  $c_{additive} = 0.05$  g/L with changing the supersaturation  $S$  in the range 2–5; the second series comprises experiments carried out at a fixed supersaturation and additive concentration, and namely  $S = 4.32$  and  $c_{additive} = 0.05$  g/L, while varying the temperature in the range 15–35 °C (precisely,  $T = 15, 25, 35$  °C). Figure 3 reports all the tests belonging to the first experimental series, showing the dependence of induction period on supersaturation at  $T = 25$  °C. Figure 3 shows that the induction period for gypsum nucleation continuously decreases with increasing supersaturation. Mostly, this figure prove that NTMP is the additive that mostly increases the induction period, thus retarding the nucleation, followed by citric acid and then by PBTC. This last, at least in the tested experimental conditions, does not augment a lot the induction period values with respect to the absence of any additive.

Experimental data belonging to the second series were used to estimate the activation energy for gypsum nucleation according to an Arrhenius relationship:

$$t_{ind} = A \exp\left(-\frac{E_{act}}{RT}\right) \quad (4)$$

where  $A$  is a constant,  $R$  the gas constant and  $E_{act}$  the activation energy.

In particular Eq.(4) was reported as a continuous line in Figure 4, and from the slopes of these straight lines the values of activation energies have been estimated. The procedure has been repeated for different supersaturation levels, and the averaged values reported in Table 1 have been obtained. The analysis of the Table reveals that if compared with the baseline (*i.e.* the  $E_{act}$  value obtained in the absence of any additive,  $E_{act} = 30$  kJ/mol, (Lancia et al., 1999)), the activation energies obtained in the presence of CA and NTMP from (Prisciandaro et al., 2005) and later (Prisciandro et al., 2009) are quite similar, while the value obtained in the presence of PBTC (Prisciandaro et al., 2012) is higher; this circumstance is quite unexpected, since PBTC is the less active in retarding gypsum nucleation among the testes additives. This has been explained with a change in nucleation mechanism, which passes from the nucleation controlled one to a growth controlled one, characterized by a higher activation energy (Prisciandaro et al., 2012).

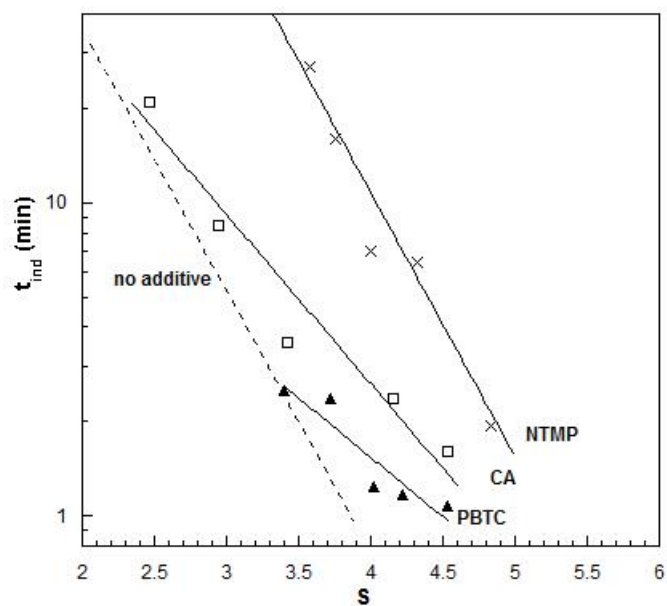


Figure 3: Induction times for gypsum nucleation as a function of  $S$ .  $T=25^{\circ}\text{C}$ ,  $c_{\text{additive}}=0.05$  g/L. -----: no additive;  $\square$ : citric acid;  $\Delta$ : PBTC;  $\times$ : NTMP

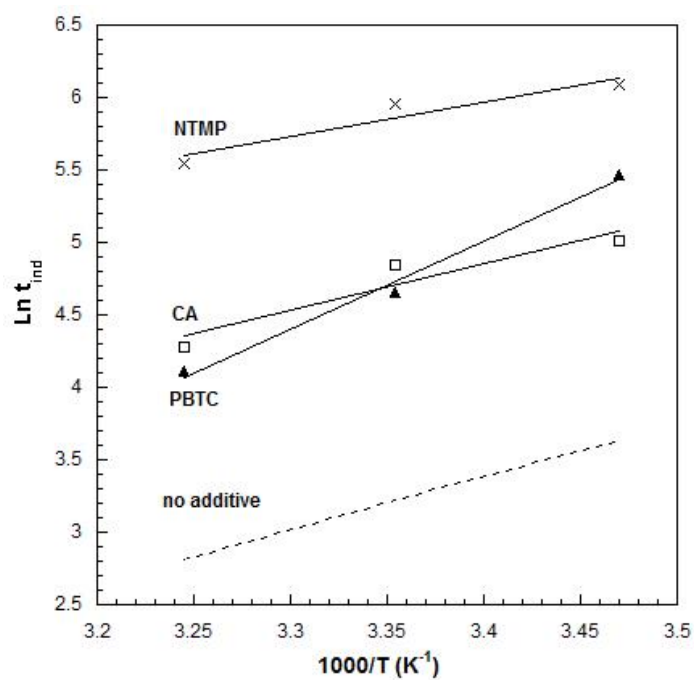


Figure 4: Induction period as a function of the inverse of temperature for  $c_{\text{additive}}=0.05$  g/L,  $S=4.32$ . -----: no additive;  $\square$ : citric acid;  $\Delta$ : PBTC;  $\times$ : NTMP.

Table 1: Estimated values for  $E_{act}$  at  $C_{additive}=0.05$  g/L (averaged on a supersaturation range  $2 < S < 4$ )

Additive	$E_{act}$ [kJ/mol]
Baseline	30
NTMP	26
CA	29
PBTC	50

#### 4. Conclusions

In this paper, the effect of different additives (CA, NTMP, PBTC) on gypsum nucleation kinetics is studied at  $T=15, 25$  and  $35$  °C and at additive concentration equal to  $0.05$  g/L. Experimental results have been used to compare the inhibiting effect of different additives on gypsum nucleation and to estimate the activation energy for the nucleation process at various additive concentrations. The results confirm that NTMP is the most active of the tested additives; moreover, the comparison among the activation energies estimated with different additives in solution, has shown that when PBTC is present, the mechanism controlling nucleation kinetic changes, passing from a nucleation controlled induction period to a growth controlled induction period.

#### References

- Kirk-Othmer Encyclopedia of Chemical Technology, 2011, Lancia, A., D. Musmarra, Prisciandaro, M. "Calcium sulfate" 1-22. Fifth Edition 2011, John Wiley & Sons, New York, USA.
- Lancia A., Musmarra D., Prisciandaro M., 1999, Measurement of the induction period for calcium sulfate dihydrate precipitation. *AIChE J.*, 45, 390-397.
- Loliou M.G., Paraskeva C.A., Koutsoukos P.G., Payatakes A.C., 2006, Calcium sulfate precipitation in the presence of water-soluble polymers. *J. Coll. Int. Sci.*, 303, 164–170.
- Marshall W.L., Slusher R., 1966, Thermodynamics of calcium sulfate dihydrate in aqueous sodium chloride solutions 0-110°. *J. Phys. Chem.*, 70, 4015-4027.
- Mullin, J.W., 2001, *Crystallization*, 4th edition, Butterworth-Heinemann Ltd, Oxford. UK.
- Prisciandaro M., Olivieri E., Lancia A., Musmarra D., 2009, Retardant effect of different additives on gypsum nucleation, *Chemical Engineering Transactions Series*, 17, 669-674.
- Prisciandaro M., Lancia A., Musmarra D., 2003, The retarding effect of citric acid on calcium sulfate nucleation kinetics. *Ind. Eng. Chem. Res.*, 42, 6647-6652.
- Prisciandaro M., Olivieri E., Lancia A., Musmarra D., 2006, Gypsum precipitation from an aqueous solution in the presence of nitrilotrimethylenephosphonic acid. *Ind. Eng. Chem. Res.*, 45, 2070-2076.
- Prisciandaro M., Olivieri E., Lancia A., Musmarra D., 2009, Gypsum Scale Control by Nitrilotrimethylenephosphonic Acid. *Ind. Eng. Chem. Res.*, 48, 10877–10883.
- Prisciandaro M., Olivieri E., Lancia A., Musmarra D., 2012, PBTC as an Antiscalant for Gypsum Precipitation: Interfacial Tension and Activation Energy Estimation, *Ind & Eng.Chem.Res.*, 51, 12844-12851.
- Prisciandaro M., Santucci A., Lancia A., Musmarra D., 2005, Role of Citric Acid in Delaying Gypsum Precipitation, *Canadian Journal of Chemical Engineering*, 83, 586-592.
- Sandhya S., Sureshbabu S., Varma H.K., Komath M., 2012, Nucleation kinetics of the formation of low dimensional calcium sulfate dihydrate crystals in isopropyl alcohol medium, *Cryst. Res. Technol.*, 47, 780–792.
- Söhnel O., J. Garside, 1992, *Precipitation*, Butterworth-Heinemann Ltd, Oxford, UK
- Söhnel O., Mullin J.W., 1988, Interpretation of crystallization induction periods *J. Coll. Int. Sci.*, 123, 43-50.